

Renewable Energy Forecasting with Echo State Networks

Samuel G. Dotson^{a,*}, Kathryn D. Huff^a

^aDept. of Nuclear, Plasma, and Radiological Engineering, University of Illinois at Urbana-Champaign, Urbana, IL 61801

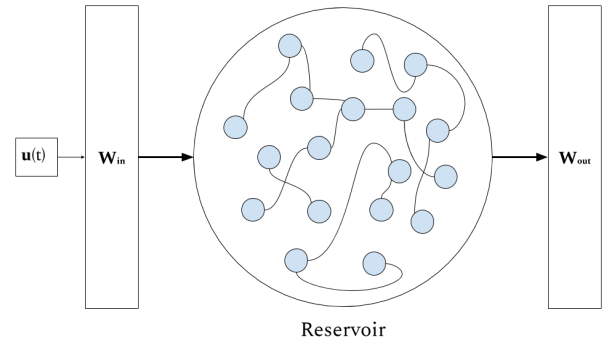
Abstract

The abstract goes here. As a general guide, you should provide a concise (150-250 words) summary of your article - introduction, methodology, results, and conclusion. Avoid using abbreviations and acronyms unless the abbreviation/acronym is used repeatedly in the abstract. There should be no references in the abstract.

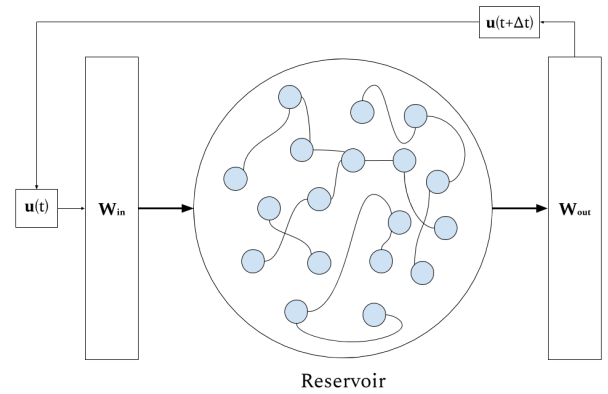
Keywords: FIXME, key words, go here, like:, simulation, spent nuclear fuel

1. Introduction

Reducing carbon emissions has become a priority for many countries in response to the rising threat of climate change. The goal set by the 2015 Paris Agreement is to prevent the global temperature from rising more than 1.5 °C above pre-industrial levels [1]. Virtually all current plans to reduce carbon emissions depend on increasing the share of energy production by renewable and clean energy sources, especially solar and wind energy [2, 3]. While solar and wind are low-carbon sources, these forms of electricity generation are variable and unpredictable. This variability is found to be major cause of black-outs and power system failures [4]. Further, even modest penetrations of renewable energy negatively affect the economics of other types of clean energy, such as nuclear power [2, 5]. There has been some work done to quantify the economic benefit of improving forecasts of renewable energy [6, 7, 8]. Some of the benefits of improving forecasts are: 1) It is often cheaper than building storage devices [6]. 2) Would reduce curtailment and allow for efficient use of non-renewable sources [7]. 3) Enable a slight, but important, amount of load-following from nuclear and bio-mass generators which are not designed for rapid load following [8].



(a) Training Flow



(b) Predicting Flow

Figure 1: Reservoir behavior in the training and predicting phases.

2. Methodology

2.1. Echo State Networks

An Echo State Network (ESN), sometimes called a “reservoir computer,” [9, 10, 11] is a type of recurrent neural network that replaces the many hidden layers of a conventional feed-forward neural network with a reservoir that is

1. sparse.
2. connected by uniformly random weights, centered at zero.
3. large (i.e. has many neurons).

The reservoir is therefore a randomly instantiated adjacency matrix, \mathbf{W} , of size $N \times N$. The input vector, $U(t)$, of K units is mapped onto the reservoir by an input matrix, W^{in} of size $N \times K$. The activation states of the reservoir are calculated by

$$x(t) = \tanh(W^{in} \cdot U(t) + \mathbf{W}x(t-1)) \quad (1)$$

Where $x(t)$ is the collection of reservoir activations [12, 10, 13]. The output is read by an output weight matrix, W^{out} .

$$y(t) = (W^{out})^T \cdot x(t) \quad (2)$$

In the training phase, the output, $U(t + \Delta t)$, is discarded and the next training input passed to the network. During the prediction phase, the output is kept and used as the next input. This behavior is shown in Figure 1. The speed of ESNs is owed to this structure; only W^{out} has tunable weights. Everything else is fixed. In this work, we adapted the open source Python package `pyESN` [14] to construct and train the network.

2.2. Hyper-parameter Optimization

ESNs are fast because the hidden layer in a conventional feed-forward neural network is replaced by a large reservoir that does not require training. The trade off is that ESNs are sensitive to various hyper-parameters that need to be optimized [13]. These hyper-parameters are summarized in Table 1. The spectral radius (ρ) should satisfy the “echo state property” which means that previous reservoir activations have a decaying influence on future states. This is usually guaranteed for $\rho < 1$, but this is not a requirement [13].

The hyper-parameters are optimized by performing a grid search over the test values specified in Table 1. The following steps were taken for each prediction task:

1. Select a hyper-parameter or pair of parameters.
2. Generate ESN prediction with the specified parameters.
3. Calculate and record the RMSE.
4. Continue until last entry in the parameter set is reached.
5. Set the network parameters to hyper-parameter value that minimizes the RMSE.

This algorithm generates an error surface where the coordinates of the absolute minimum correspond to the indices of values in the hyper-parameter test sets that minimized the RMSE.

2.3. Prediction Tasks

We first performed a benchmarking task by making a prediction for the Lorenz 1963 model [15]. Then we optimized predictions for univariate time-series representing total demand, solar energy, and wind energy 4-hours ahead and 48- hours ahead. Finally, those same six tasks are repeated with an additional predictor. The tasks are summarized in Table 2.

2.4. Data Selection

All data predicting demand, wind energy, and solar energy on the University of Illinois at Urbana-Champaign (UIUC) campus are from the UIUC Solar Farm 1.0 dashboard [16] and proprietary data shared with us courtesy of the UIUC Facilities and Services Department. All data had hourly resolution. Weather data was retrieved from the National Oceanic and Atmospheric Administration (NOAA)[17] for two locations: Champaign, IL, where UIUC is located, and Lincoln, IL, where Railsplitter Windfarm is located. UIUC has a power purchase agreement with Railsplitter Windfarm [18]. In the case of UIUC solar data, significant portions were missing due to instrument failure. In order to fill in this missing data, we calculated the theoretical solar energy production based on irradiance data from OpenEI [19]. The solar output is given by [20]

$$P = G_T \eta_{ref} \tau_{pv} A [1 - \gamma (T - 25)] [W] \quad (3)$$

*Corresponding Author

Email address: `sgd2@illinois.edu` (Samuel G. Dotson)

Table 1: Description of Model Hyper-parameters

Hyper-parameter	Purpose	Tested Values
noise	Neuron regularization	[0.0001, 0.0003, 0.0007, 0.001, 0.003, 0.005, 0.007, 0.01]
ρ	Spectral radius	[0.5, 0.7, 0.9, 1, 1.1, 1.2, 1.3, 1.5]
N	Size of reservoir, W	[600, 800, 1000, 1500, 2000, 2500, 3000, 4000]
sparsity	The density of connections in W	[0.005, 0.01, 0.03, 0.05, 0.1, 0.12, 0.15, 0.2]
Training Length	Size of the training set before prediction	$L \in [5000, 25000]$, step size = 300

Table 2: Summary of Prediction Tasks

Target	Future	Additional Predictor
Total Demand	4 hours ahead	None
Solar Energy		Solar Elevation Humidity Pressure
Wind Energy	48 hours ahead	Wet Bulb Temp. Dry Bulb Temp. Wind Speed

where

$$G_T = P_{DNI} * \cos(\beta + \delta - lat) + P_{DHI} * \left(\frac{180 - \beta}{180}\right) \left[\frac{W}{m^2}\right] \quad (4)$$

where

$$\delta = 23.44 \sin\left(\left(\frac{\pi}{180}\right) \left(\frac{360}{365}\right) (N + 284)\right) [\text{degrees}] \quad (5)$$

η, τ, γ are solar panel properties

P_{DNI} is the direct normal irradiance

P_{DHI} is the diffuse horizontal irradiance

β is the tilt angle of the solar panels

The solar elevation angle, α , was also calculated [21, 22] using coordinates for the UIUC solar farm.

$$\alpha = \sin^{-1} [\sin(\delta) \sin(\phi) + \cos(\delta) \cos(\phi) \cos(\omega)] \quad (6)$$

where

δ is the declination angle

ϕ is the latitude of interest

ω is the hour angle

3. Results

3.1. Benchmark: Lorenz 1963

We first verified that our choice of implementation for ESNs produces similar results to those found in the literature [9]. The hyper-parameters that

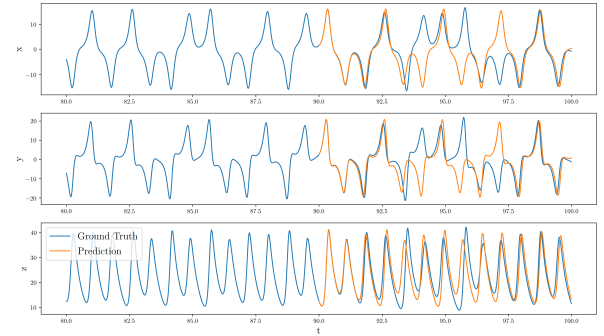


Figure 2: Using an ESN to replicate the climate of the Lorenz Attractor.

minimized the RMSE of the model can be found in Table 3. Our optimized values are somewhat different from the literature, but we are satisfied that our ESN has successfully replicated the climate of the Lorenz Attractor similar to Pathak et. al 2017.

Table 3: Hyper-parameters for the Lorenz 1963 Model

Parameter	This paper	Literature [9]
N	2000	300
ρ	0.9	1.2
sparsity	0.1	0.1
noise	0.001	0
Training Length	3200	Not Specified

4. Acknowledgments

This work was made possible with the support from the people at UIUC Facilities & Services. In particular, Morgan White, Mike Marquissee, and Mike Larson. It was also aided by other members of the Advanced Reactors and Fuel Cycles (ARFC) group, in particular Nathan Ryan. This work is supported by the Nuclear Regulatory Commission Fellowship Program. Prof. Huff is supported by the Nuclear Regulatory Commission Faculty Development Program (award NRC-HQ-84-14-G-0054 Program B), the Blue Waters sustained-petascale computing project supported by the National Science Foundation (awards OCI-0725070 and ACI-1238993) and the state of Illinois, the DOE ARPA-E MEITNER Program (award DE-AR0000983), and the DOE H2@Scale Program (Award Number: DE-EE0008832)

References

- [1] The paris agreement | UNFCCC.
URL <https://unfccc.int/process-and-meetings/the-paris-agreement/the-paris-agreement>
- [2] C. Cany, C. Mansilla, G. Mathonnière, P. da Costa, Nuclear contribution to the penetration of variable renewable energy sources in a french decarbonised power mix 150 544–555. doi:10.1016/j.energy.2018.02.122.
URL <http://www.sciencedirect.com/science/article/pii/S0360544218303566>
- [3] J. Chilvers, T. J. Foxon, S. Galloway, G. P. Hammond, D. Infield, M. Leach, P. J. Pearson, N. Strachan, G. Strbac, M. Thomson, Realising transition pathways for a more electric, low-carbon energy system in the united kingdom: Challenges, insights and opportunities 231 (6) 440–477, publisher: IMECHE. doi:10.1177/0957650917695448.
URL <https://doi.org/10.1177/0957650917695448>
- [4] H. Haes Alhelou, M. E. Hamedani-Golshan, T. C. Njenda, P. Siano, A survey on power system black-out and cascading events: Research motivations and challenges 12 (4) 682, number: 4 Publisher: Multidisciplinary Digital Publishing Institute. doi:10.3390/en12040682.
URL <https://www.mdpi.com/1996-1073/12/4/682>
- [5] J. H. Keppler, C. Marcantonini, O. N. E. Agency, O. for Economic Co-operation {and} Development, Carbon pricing, power markets and the competitiveness of nuclear power, Nuclear development, Nuclear Energy Agency, Organisation for Economic Co-operation and Development.
- [6] Q. Wang, C. B. Martinez-Anido, H. Wu, A. R. Florita, B.-M. Hodge, Quantifying the economic and grid reliability impacts of improved wind power forecasting 7 (4) 1525–1537, conference Name: IEEE Transactions on Sustainable Energy. doi:10.1109/TSSTE.2016.2560628.
- [7] E. V. Mc Garrigle, P. G. Leahy, Quantifying the value of improved wind energy forecasts in a pool-based electricity market 80 517–524. doi:10.1016/j.renene.2015.02.023.
URL <http://www.sciencedirect.com/science/article/pii/S0960148115001135>
- [8] C. Brancucci Martinez-Anido, B. Botor, A. R. Florita, C. Draxl, S. Lu, H. F. Hamann, B.-M. Hodge, The value of day-ahead solar power forecasting improvement 129 192–203. doi:10.1016/j.solener.2016.01.049.
URL <http://www.sciencedirect.com/science/article/pii/S0038092X16000736>
- [9] J. Pathak, Z. Lu, B. R. Hunt, M. Girvan, E. Ott, Using machine learning to replicate chaotic attractors and calculate lyapunov exponents from data 27 (12) 121102. arXiv:1710.07313, doi:10.1063/1.5010300.
URL <http://arxiv.org/abs/1710.07313>
- [10] J. Pathak, B. Hunt, M. Girvan, Z. Lu, E. Ott, Model-free prediction of large spatiotemporally chaotic systems from data: A reservoir computing approach 120 (2) 024102, publisher: American Physical Society. doi:10.1103/PhysRevLett.120.024102.
URL <https://link.aps.org/doi/10.1103/PhysRevLett.120.024102>
- [11] P. R. Vlachas, J. Pathak, B. R. Hunt, T. P. Sapsis, M. Girvan, E. Ott, P. Koumoutsakos, Backpropagation algorithms and reservoir computing in recurrent neural networks for the forecasting of complex spatiotemporal dynamics 126 191–217. doi:10.1016/j.neunet.2020.02.016.
URL <http://www.sciencedirect.com/science/article/pii/S0893608020300708>
- [12] G. Shi, D. Liu, Q. Wei, Energy consumption prediction of office buildings based on echo state networks 216 478–488. doi:10.1016/j.neucom.2016.08.004.
URL <http://www.sciencedirect.com/science/article/pii/S0925231216308219>
- [13] M. Lukoševičius, A practical guide to applying echo state networks, in: G. Montavon, G. B. Orr, K.-R. Müller (Eds.), Neural Networks: Tricks of the Trade: Second Edition, Lecture Notes in Computer Science, Springer, pp. 659–686. doi:10.1007/978-3-642-35289-8_36.
URL https://doi.org/10.1007/978-3-642-35289-8_36
- [14] C. Korndörfer, pyESN.
URL <https://github.com/cknd/pyESN>
- [15] E. N. Lorenz, Deterministic nonperiodic flow 20 (2) 130–141, publisher: American Meteorological Society Section: Journal of the Atmospheric Sciences. doi:10.1175/1520-0469(1963)020<0130:DNF>2.0.CO;2.
URL https://journals.ametsoc.org/view/journals/atsc/20/2/1520-0469_1963_020_0130_dnf_2_0_co_2.xml
- [16] AlsoEnergy, University of illinois solar farm dashboard,

Table 4: Tabulated error for 48-hour ahead total electricity demand forecasts with various coupled quantities. Improvement indicates the percentage improvement over the base case of forecasting electricity demand alone.

Scenario	MAE	RMSE	Improvement MAE (%)	Improvement RMSE (%)
Total Demand	0.018892	0.024137	[-]	[-]
Demand + Sun Elevation	0.013375	0.022893	-29.20	-5.15
Demand + Humidity	0.048357	0.063544	+155.96	+163.26
Demand + Pressure	0.009329	0.017334	-50.62	-28.18
Demand + Wet Bulb Temp.	0.033473	0.039922	+77.18	+65.40
Demand + Dry Bulb Temp.	0.031866	0.040409	+66.67	+67.42
Demand + Wind Speed	0.051045	0.074966	+170.19	+210.58

Table 5: Tabulated error for 4-hour ahead total electricity demand forecasts with various coupled quantities. Improvement indicates the percentage improvement over the base case of forecasting electricity demand alone.

Scenario	MAE	RMSE	Improvement MAE (%)	Improvement RMSE (%)
Total Demand	0.019343	0.026322	[-]	[-]
Demand + Sun Elevation	0.009869	0.016928	-48.98	-35.69
Demand + Humidity	0.054772	0.073056	+183.16	+177.54
Demand + Pressure	0.009754	0.019314	-49.57	-26.62
Demand + Wet Bulb Temp.	0.020932	0.026979	+8.21	+2.50
Demand + Dry Bulb Temp.	0.026577	0.039963	+37.40	+51.82
Demand + Wind Speed	0.042534	0.067427	+119.89	+156.16

<http://s35695.mini.alsoenergy.com/Dashboard/2a5669735065572f4a42454b772b714d3d>.

- URL <http://s35695.mini.alsoenergy.com/Dashboard/2a5669735065572f4a42454b772b714d3d>
- [17] N. C. for Environmental Information, Find a station | data tools | climate data online (CDO) | national climatic data center (NCDC).

URL <https://www.ncdc.noaa.gov/cdo-web/datatools/findstation>

- [18] S. Breitweiser, Wind power: University of illinois at urbana-champaign.

URL https://www.fs.illinois.edu/docs/default-source/news-docs/newsrelease_windppa___factsheet.pdf?sfvrsn=43aaffea_0

- [19] National solar radiation data base - NSRDB viewer - OpenEI datasets.

URL <https://openei.org/datasets/dataset/national-solar-radiation-data-base/resource/b2074dd9-36a4-4382-a12f-e795b578404c>

- [20] H. E. Garcia, J. Chen, J. S. Kim, M. G. McKellar, W. R. Deason, R. B. Vilim, S. M. Bragg-Sitton, R. D. Boardman, Nuclear hybrid energy systems regional studies: West texas & northeastern arizona. doi:10.2172/1236837.

URL <https://www.osti.gov/biblio/1236837-nuclear-hybrid-energy-systems-regional-studies-west-texas-northeastern-arizona>

- [21] N. US Department of Commerce, ESRL global monitoring laboratory - global radiation and aerosols.

URL <https://www.esrl.noaa.gov/gmd/grad/solcalc/calcdetails.html>

- [22] J. Meeus, Astronomical Algorithms, 2nd Edition, Willmann-Bell, Inc.

Table 6: Tabulated error for 48-hour ahead solar energy forecasts with various coupled quantities. Improvement indicates the percentage improvement over the base case of forecasting solar energy alone.

Scenario	MAE	RMSE	Improvement MAE (%)	Improvement RMSE (%)
Solar Energy	0.143276	0.206162	[-]	[-]
Solar + Sun Elevation	0.200627	0.292516	+40.02	+41.88
Solar + Humidity	0.086920	0.111476	-39.33	-45.93
Solar + Pressure	0.098554	0.152672	-31.21	-25.94
Solar + Wet Bulb Temp.	0.114157	0.167503	-20.32	-18.75
Solar + Dry Bulb Temp.	0.079036	0.123783	-44.84	-39.96
Solar + Wind Speed	0.147270	0.191722	+2.788	-7.004

Table 7: Tabulated error for 4-hour ahead solar energy forecasts with various coupled quantities. Improvement indicates the percentage improvement over the base case of forecasting solar energy alone.

Scenario	MAE	RMSE	Improvement MAE (%)	Improvement RMSE (%)
Solar Energy	0.061426	0.095794	[-]	[-]
Solar + Sun Elevation	0.033263	0.060048	-45.85	-37.32
Solar + Humidity	0.054951	0.078739	-10.54	-17.80
Solar + Pressure	0.046862	0.089294	-23.71	-6.78
Solar + Wet Bulb Temp.	0.038104	0.053419	-37.97	-44.24
Solar + Dry Bulb Temp.	0.044104	0.073112	-28.20	-23.68
Solar + Wind Speed	0.070293	0.099912	+14.44	+4.30

Table 8: Tabulated error for 48-hour ahead wind forecasts with various coupled quantities. Improvement indicates the percentage improvement over the base case of forecasting wind energy alone.

Scenario	MAE	RMSE	1 MAE (%)	Improvement RMSE (%)
Wind Energy	0.103516	0.130848	[-]	[-]
Wind + Sun Elevation	0.051899	0.081339	-49.82	-37.84
Wind + Humidity	0.091975	0.112054	-11.15	-14.36
Wind + Pressure	0.054388	0.097670	-47.46	-25.36
Wind + Wet Bulb Temp.	0.074085	0.097004	-28.43	-25.86
Wind + Dry Bulb Temp.	0.081268	0.105289	-21.49	-19.53
Wind + Wind Speed	0.100880	0.122271	-2.5464	-6.555

Table 9: Tabulated error for 4-hour ahead wind forecasts with various coupled quantities. Improvement indicates the percentage improvement over the base case of forecasting wind energy alone.

Scenario	MAE	RMSE	Improvement MAE (%)	Improvement RMSE (%)
Wind Energy	0.090266	0.124303	[-]	[-]
Wind + Sun Elevation	0.039248	0.083134	-56.52	-33.12
Wind + Humidity	0.064131	0.096310	-28.95	-22.52
Wind + Pressure	0.043739	0.087981	-51.54	-29.22
Wind + Wet Bulb Temp.	0.044447	0.077770	-50.76	-37.44
Wind + Dry Bulb Temp.	0.050536	0.083151	-44.01	-33.11
Wind + Wind Speed	0.063456	0.088157	-29.70	-29.07